MAXIMUM ALLOWABLE CRACK SIZE FOR CRACKS IN THE ATTACHMENT WELD OF NUCLEAR STEAM GENERATOR UPPER LATERAL SUPPORT LUGS

Songyan (S.-Y.) Yang*, Alice Sze
Ontario Power Generation – Nuclear, 889 Brock Road, Pickering, Ontario, Canada L1W 3J2
* Corresponding author, telephone: (905) 839 6746 ext. 5199, E-mail: songyan.yang@opg.com

Abstract

Crack indications in the steam generator upper lateral support lug attachment welds were conservatively analyzed using two models: beam-bending model and semi-spherical shell model. In both models, analyses were performed based on the most severe design loadings (Level D loads), including the appropriate ASME structural factors. Linear elastic fracture mechanic (LEFM) with Irwin crack tip plastic zone correction and small scale yielding (SSY) was adopted to establish critical crack sizes. The critical crack sizes were used to dispose of inspected crack indications that exceeded the ASME code Section XI subarticle IWB-3500 acceptance criteria.

1. Introduction and description of problem

In Fall 2005, periodic inspections of Darlington Unit 4 steam generators (SG) were performed on the external shell using magnetic particle inspections. The inspection included seven of the main support lug attachment welds and five of the upper lateral restraint lug attachment welds. Among all these inspected locations, two crack indications were reported: one is 12 mm long and the other is 35 mm long. The two reported crack indications, which surpassed the acceptance criteria of ASME code Section XI Table IWB-3510-3 [1] are the subject of this paper. Sketches and picture of these two crack indications are illustrated in Figure 1 and Figure 2. A schematic diagram of the lateral support lug with the location of the crack indications identified is given in Figure 3.

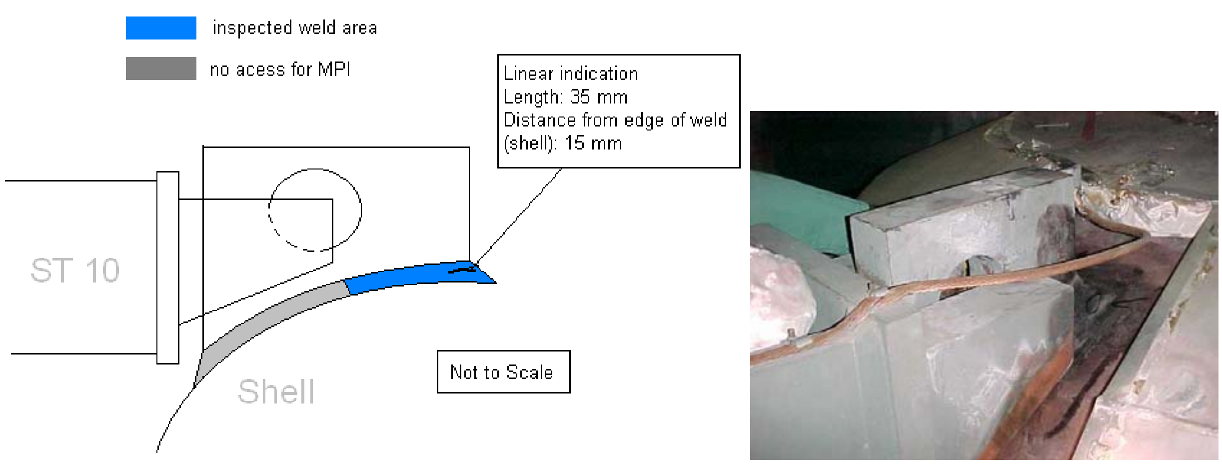

Figure 1 Inspection sketch and picture of crack indications on lug ST10 of SG BO1

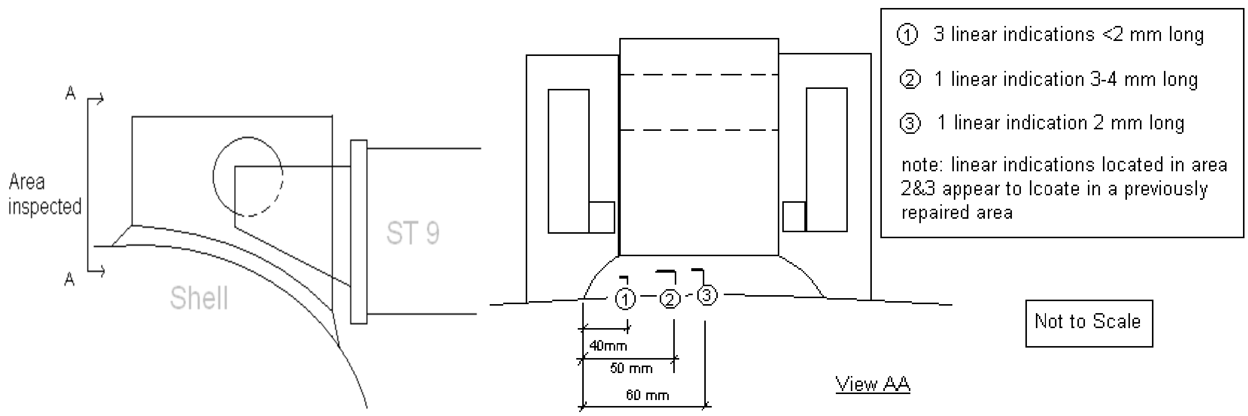

Figure 2 Inspection sketch of crack indications on lug ST9 of SG BO4

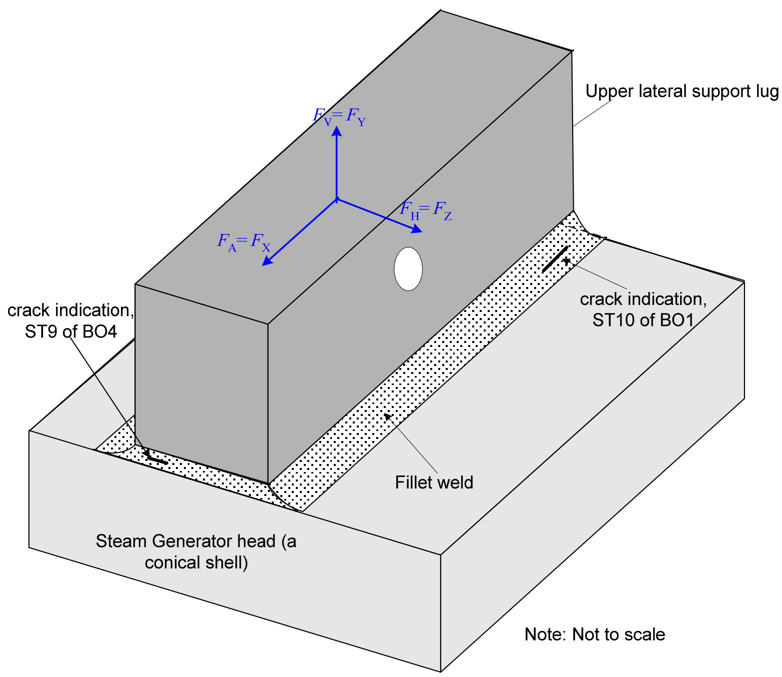

Figure 3 Schematic illustration of crack indication, lateral support lug and fillet weld

The 35 mm long crack indication was detected in ST10 of BO1. This crack indication is located within the attachment weld and is oriented parallel to the weld edge. Five short crack indications, each less than 4mm long, were detected in ST9 of BO4. The five crack indications are located within the attachment weld and are oriented parallel to the weld edge. Due to the proximity of the cracks, based on the sizing criterion for linear flaws (ASME code Section XI subarticle IWA-3400), the five crack indications might be combined to give an overall length of 12 mm. The two crack sizes were then checked against the acceptance criteria of ASME code Section XI Table IWB-3510-3. It was found that the 35 mm crack indication well exceeds the allowable crack size and the combined 12 mm one barely meets the allowable crack size.

Fracture mechanics analysis was performed to determine acceptable crack sizes that would ascertain stability of cracks in the attachment welds. The two crack indications were then compared with the calculated critical crack sizes to determine the fitness-for-service of the attachment welds.

2. Assumptions, simplifications, and limitations

Two calculations models, beam-bending calculation model and semi-spherical shell calculation model, were used to determine an acceptable crack depth. The following assumptions and simplifications are applicable to the beam-bending calculation model:

a. Cracks are planar and are located under the support lugs. Length of crack in B01 ST10 is equal to the length of the support lug; whereas crack in B04 ST9 is equal to the width of the support lug. Both crack faces are on the outside tangential plane of the SG head (a conical shell). These assumption are conservative in that i) crack lengths are exaggerated significantly, and ii) the most severe failure mode of crack, i.e. mode I failure is simulated.

b. The magnitude of load (force) is the vector addition of applied forces on the support lug. Directions of load for the postulated cracks yield Mode I (cleavage) failure.

c. Load due to internal pressure is negligible because stress components that are parallel to the crack face has a much smaller effect on crack driving force than that perpendicular to it in most cases.

d. Stress is calculated based on beam-bending theory.

The following assumptions and simplifications are applicable to the semi-spherical shell calculation model:

a. Cracks are planar and perpendicular to and on the outside surface of SG head. Crack face either along or perpendicular to the meridian plane of SG head is considered.

b. Load is purely due to internal pressure of SG. Design pressure is used.

c. Load due to beam bending is not considered.

The following assumptions and simplifications are applicable to both models:

a. Residual stress due to welding is negligible because all welds were stress-relieved by post weld heat treatment (PWHT) (Section 2.1 of reference [6]).

b. Mode I stress intensity factor (SIF) is chosen as the crack driving force. Effect of crack tip plastic zone is considered via plane stress form of Irwin plastic zone correction. The calculation of margin on SIF is based on “effective” rather than original SIF.

c. Crack stability is achieved when margins on both SIF and stress are larger than one. This assumption is conservative because strain hardening of material is not considered in calculation. Should strain hardening be considered, a) the margin on stress would increase; and b) the size of crack tip plastic zone would decrease, which would result in a smaller crack driving force.

d. Level D loading conditions and structural factors of ASME Section XI Article H-4200 [1] are considered.

e. Material properties are taken from Pipe Fracture Encyclopedia [3]. Minimum values of (initial) yield strength and fracture toughness at crack initiation J_{IC} are chosen in the calculation when multiple test data are available.

3. Evaluation procedure and definition of margins

3.1 Evaluation procedure

Evaluation procedure of stability of cracks is illustrated in Figure 4. The evaluation was based on linear elastics fracture mechanic (LEFM) theory so that:

- Mode I SIF is the crack driving force.
- Plain strain SIF at crack initiation K_{IC} is the material's fracture toughness.
- Plane stress form of Irwin Crack tip plastic zone correction is adopted in the calculation of maximum crack size.
- Small scale yielding (SSY) is ensured throughout the evaluation.

For the applicability of LEFM with SSY, the following equations must be satisfied at any stage of evaluation:

$$K_{\mathrm{I}}(a_{\mathrm{eff}}) \le K_{\mathrm{IC}}; \qquad a_{\mathrm{eff}} = a + r_p; \qquad r_p = \frac{K_{\mathrm{I}}^2}{2\pi\sigma_y^2}$$

where a is physical crack size, a_{eff} is effective crack size considering crack tip plastic zone, r_p is radius of the plane-stress form of Irwin plastic zone circle and σ_y is yield strength. SSY requires crack tip plastic zone to be small and cracks to be surrounded by elastic material.

To ensure uncontrolled plastic deformation will not occur during the evaluation, the following equation must also be satisfied:

$$\sigma_{\mathrm{mises}} \le \sigma_y$$

where σ_{mises} is the von Mises equivalent stress calculated at the location of crack and in absence of the crack. The underlying assumption is that material is elastic perfectly plastic, i.e. strain hardening is not considered.

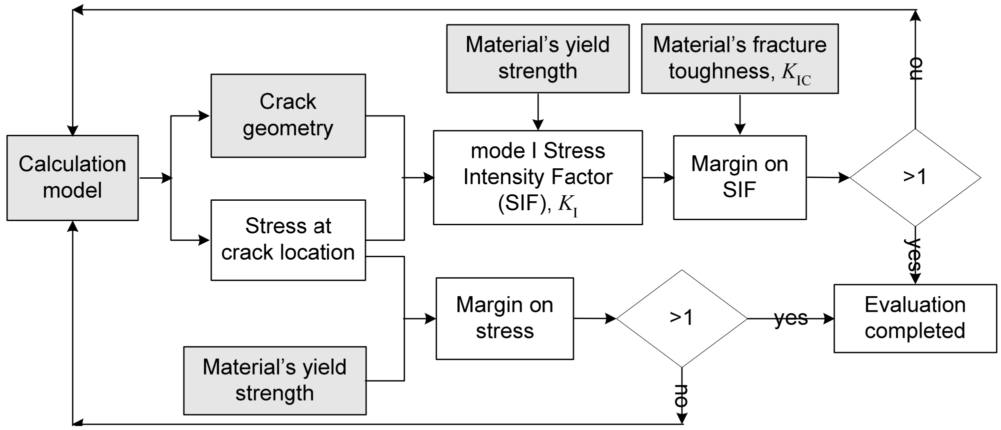

Figure 4 Evaluation procedure of stability of cracks

3.2 Definition of margins

Two margins were used to determine the stability of cracks: margin on SIF, and margin on stress. Margin on SIF is the ratio of material's fracture toughness and crack driving force whereas margin on stress is the ratio of yield strength and von Mises equivalent stress, i.e.

$$\text{Margin on SIF} = \frac{K_{\text{IC}}}{K_{\text{I}}(a_{\text{eff}})} \qquad \text{Margin on stress} = \frac{\sigma_y}{\sigma_{\text{mises}}}$$

where K_{I} is calculated based on effected crack size.

A crack is stable when both margins are greater than or equal to one, i.e.

$$\frac{K_{\text{IC}}}{K_{\text{I}}(a_{\text{eff}})} \geq 1 \text{ and } \frac{\sigma_y}{\sigma_{\text{mises}}} \geq 1$$

In order to judge whether crack tip plastic deformation has penetrated the depth of respective calculation model, plastic deformation as fraction of remaining ligament was defined below:

$$\text{For beam-bending model: } \frac{2r_p}{\min(A,B,C)-a} \qquad \text{For semi-spherical shell model: } \frac{2r_p}{t-a}$$

where a is crack depth, A, B and C are lug dimensions adopted in beam-bending calculation model, t is wall thickness for semi-spherical shell calculation model. A crack is surrounded by elastic material when the above two equations are less than one. Detail definitions of these geometry parameters are illustrated in Figure 5 and Figure 6.

3.3 Structural factors

Structural factors of ASME Section XI Article H-4200 [1] were considered in this calculation. Both forces on the lug and internal pressure on the SG head were classified as Level D loads. For Level D loading conditions, the following structural factors were used in calculation:

Membrane stress $SF_m = 1.3$ Bending stress $SF_b = 1.4$

4. Calculation methods

4.1 Beam-bending calculation model

The load acting upon the SG upper lateral support are shown in Figure 3, i.e. horizontal force F_A acting in the radial direction of SG head, horizontal force F_H acting at circumferential direction of SG head and vertical force F_V. Level D condition was considered in these forces and these three forces were the only components that affected the support stresses [2].

In the beam-bending calculation model, the support lug was conservatively modeled as a beam subjected to bending moment caused by F_A, F_H and F_V. Per reference [2], $F_\mathrm{A} = 2{,}886{,}896\,\mathrm{N}$, $F_H = 346{,}961\,\mathrm{N}$ and $F_V = -10{,}231\,\mathrm{N}$. The magnitude of force, F, was the vector addition of the three force components multiply by the bending stress structural factor, i.e.

$$F = SF_b \cdot \sqrt{F_\mathrm{A}^2 + F_\mathrm{H}^2 + F_\mathrm{V}^2}$$

The beam-bending calculation model with the dimensions of the equivalent lug is schematically shown in Figure 5.

The direction of F was conservatively rotated to a direction that would generate Mode I failure of crack. In order to obtain a realistic bending moment M, the force F was further conservatively placed on the top plane of the idealized lug. Under such loading condition, bending moment M can be expressed as

$$M = F \times A$$

Based on beam bending theory, the maximum bending stress can be expressed as

$$\sigma_{\max} = \frac{M \cdot \frac{C}{2}}{I} = \frac{F \cdot A \cdot \frac{C}{2}}{\frac{BC^3}{12}} = \frac{6F \cdot A}{B \cdot C^2}$$

For lug ST10 of BO1, single edge notched specimen with uniform far end tension $\sigma_{\max}$ as shown in Figure 5 (b) was adopted to calculate crack driving force, i.e. Mode I SIF, K_{I}, can be expressed as [4]:

$$K_{\mathrm{I}} = \sigma_{\max}\sqrt{\pi a_1} \cdot F_1(a_1, B)$$

where a_1 is the crack depth on lug ST10 of BO1, B is the width of the idealized lug and geometry correction factor $F_1(a_1, B)$ can be expressed as:

$$F_1(a_1, B) = \sqrt{\frac{2B}{\pi_1 a}\tan\left(\frac{\pi a_1}{2B}\right)}\,\frac{0.752 + 2.02\left(\frac{a_1}{B}\right) + 0.37\left[1 - \sin\left(\frac{\pi_1 a}{2B}\right)\right]^3}{\cos\left(\frac{\pi a_1}{2B}\right)}$$

For lug ST9 of BO4, single edge notched specimen with pure bending of $+\sigma_{\max}$ and $-\sigma_{\max}$ as shown in Figure 5 (c) were adopted to calculate Mode I SIF K_{I} [4]:

$$K_{\mathrm{I}} = \sigma_{\max}\sqrt{\pi a_2} \cdot F_2(a_2, C)$$

where a_2 is the crack depth on lug ST9 of BO4, C is the length of the idealized lug and geometry correction factor $F_2(a_2, C)$ can be expressed as:

$$F_2(a_2, C) = \sqrt{\frac{2C}{\pi a_2}\tan\left(\frac{\pi a_2}{2C}\right)}\,\frac{0.923 + 0.199\left[1 - \sin\left(\frac{\pi a_2}{2C}\right)\right]^4}{\cos\left(\frac{\pi a_2}{2C}\right)}$$

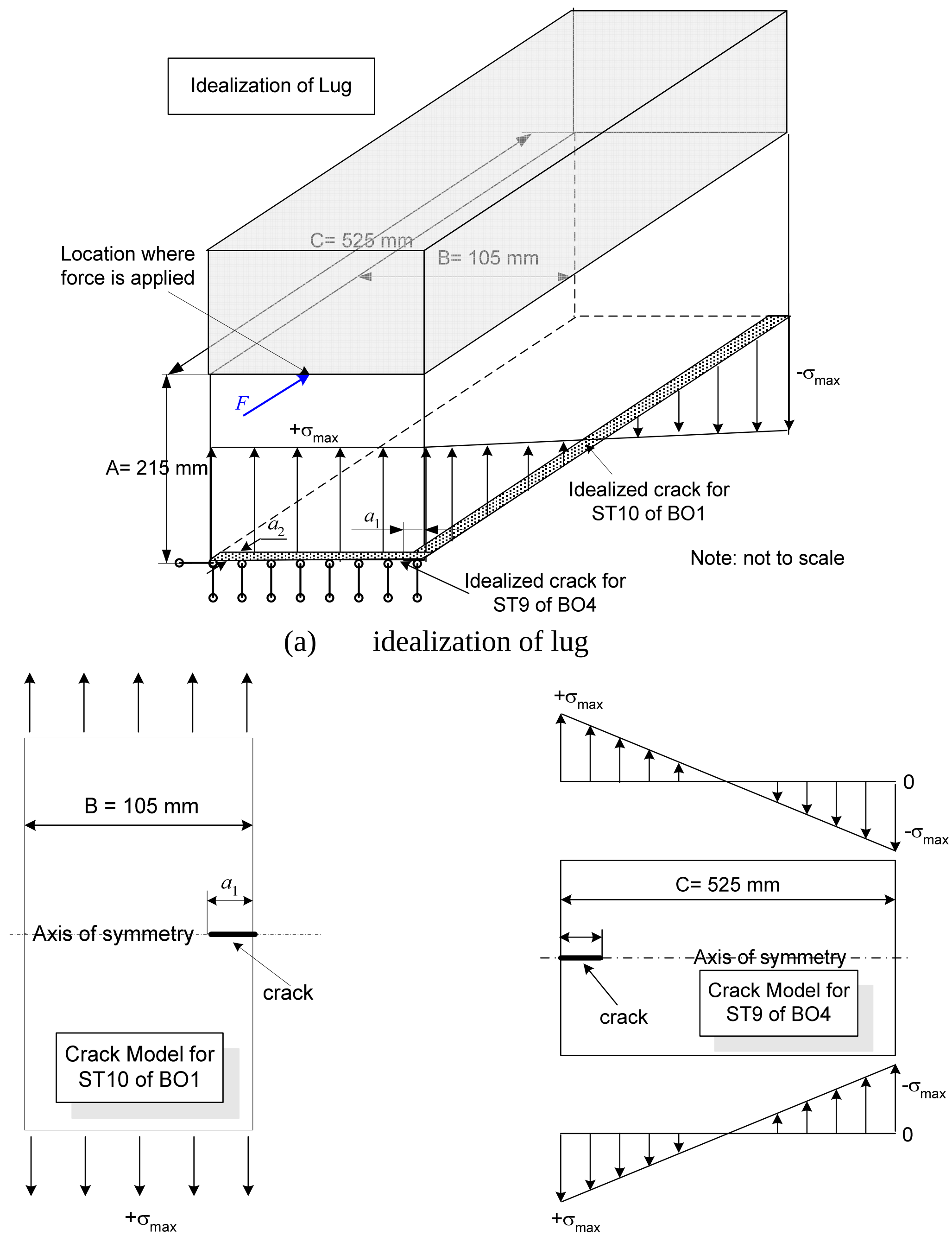

(a) idealization of lug

(b) crack model for ST10 of BO1

(c) crack model for ST9 of BO4

Figure 5 Illustration of beam-bending calculation model

4.2 Semi-spherical shell calculation model

The crack indications may also grow through the wall thickness of the SG head. In the semi-spherical shell calculation model, the SG head was ideally modeled as a semi-spherical thin-walled shell with a radius R and a wall thickness t as shown schematically in Figure 6.

Design pressure of 5.688 MPa (g) was taken from SG technical specification report. Based on thin shell theory [5], two normal stresses are generated under internal pressure, i.e. stress σ_θ perpendicular to the meridian plane, and stress σ_φ parallel to the rotation axis. The magnitude of these two stresses which are the same in magnitude can be expressed as

$$\sigma_\theta = \sigma_\varphi = \frac{p \cdot R}{2t}$$

Crack was assumed to lie on the plane perpendicular to either stress σ_θ or stress σ_φ on the outside surface of the semi-spherical shell. Model I SIF, K_I, can be expressed as [4]:

$$K_\mathrm{I} = \sigma\sqrt{\pi a}F(a,t)$$

where structural factor for membrane stress (SF_m=1.3) was used in calculating stress σ, i.e.

$$\sigma = SF_m \cdot \sigma_\theta \quad \text{or} \quad \sigma = SF_m \cdot \sigma_\varphi$$

$$F = \sqrt{\frac{2t}{\pi a}\tan\left(\frac{\pi a}{2t}\right)}\,\frac{0.752 + 2.02\left(\frac{a}{t}\right) + 0.37\left[1 - \sin\left(\frac{\pi a}{2t}\right)\right]^3}{\cos\left(\frac{\pi a}{2t}\right)}.$$

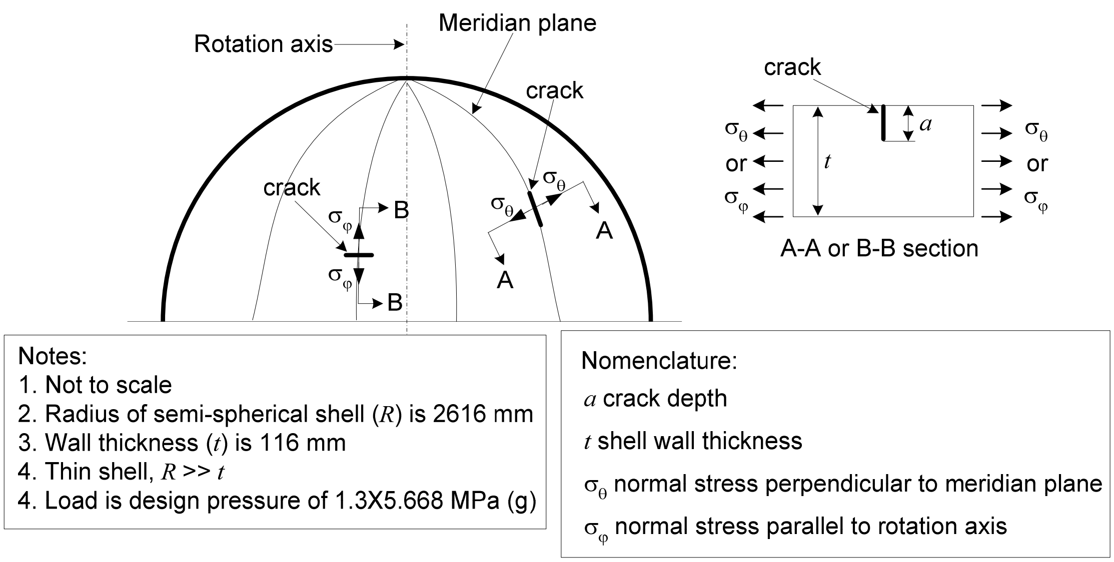

Figure 6 Illustration of semi-spherical shell calculation model

4.3 Materials Properties

The material involved in this evaluation was SA-516 Gr. 70. The material properties used in this evaluation were taken from test results compiled in reference [3], i.e. yield strength σ_y and critical plane strain SIF at crack initiation K_{IC}. When more than one test results were available for a property, the one which would generate conservative evaluation result was chosen. In this evaluation, the minimum values of both properties were used. The material properties used in this evaluation are tabulated in the following table.

Test ID	Test temperature	σ_y (MPa)	J_{IC} (kJ/m^2)	E (MPa)	K_{IC} (MPa·m$^{1/2}$)[1]
F40-1	288 °C	234.0	-	-	-
F40W-5C	288°C	-	30.1	1.8×10^5	73.6

Note 1: this value is calculated from JIC using plane-stress equation $K_{IC} = \sqrt{J_{IC}E}$ where Young's Modulus E takes 180.0 GPa.

5. Description of results

Analyses were carried out in parametric fashion. For each crack model, under a given loading condition (expressed by constant margin on stress), margins on SIF were calculated over a range of crack depth, ranging from 10 mm to 50 mm. Crack tip plastic zone expressed as fractions of remaining ligament were also calculated for each respective model. Since 10 mm and 15 mm were particularly important to inspection, the margins for these two crack configurations were highlighted in this evaluation. For other crack configurations, margins on SIF and the size of crack tip plastic deformation can be similarly determined.

5.1 Results from beam-bending calculation model

Curves of margins on SIF versus crack depth of lug ST10 of B01 and lug ST9 of B04 are shown in Figure 7. For lug ST10 B01, margin on SIF is 1.5 for a 10mm deep crack and 1.1 for a 15mm deep crack. For lug ST9 B04, the margins are 1.8 and 1.5 respectively. In both models, the margin on stress is 1.3 and does not vary with crack depths. For both crack configurations, the size of crack tip plastic zone is small in both models. So that all conditions specified in Section 3 for LEFM under SYY are satisfied.

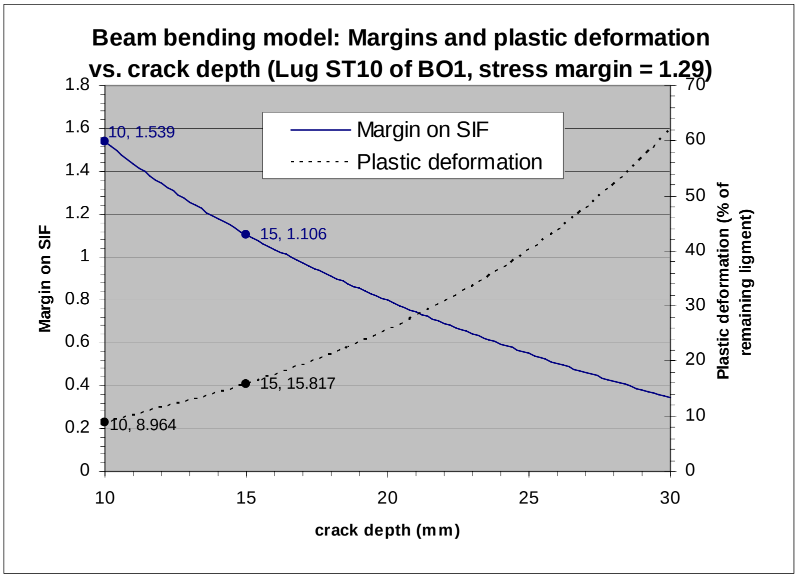

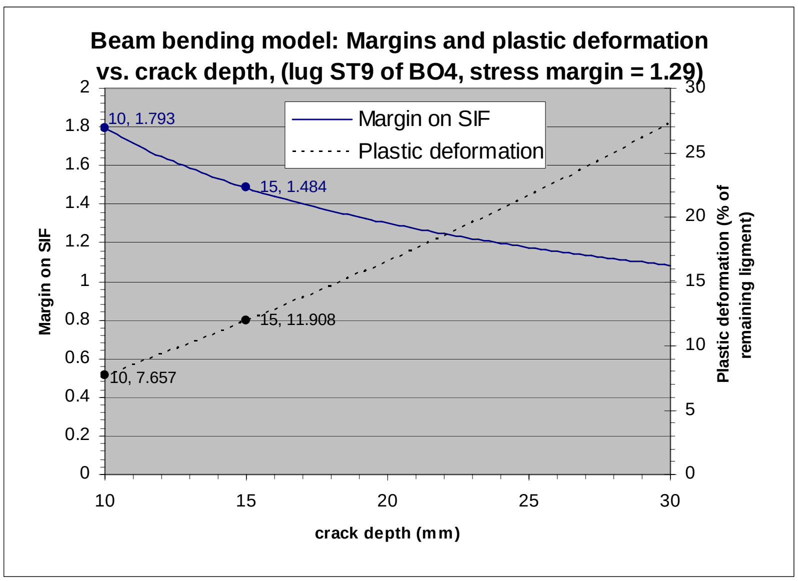

Figure 7 Analysis results according to beam bending model

5.2 Results from semi-spherical shell calculation model

A similar plot is obtained from the semi-spherical shell calculation model. Figure 8 shows that a 10 mm crack depth has a margin on SIF of 4.0, and a 15mm crack depth has a margin on SIF of 3.1. The margins on SIF are much greater than the ones obtained from the beam-bending model. The reason is due to the relatively low stress produced purely by the internal pressure of SG in semi-spherical model. Margin on stress is 2.8 which does not vary with crack depths. The size of crack tip plastic zone is small for both crack configurations as shown in Figure 8 and therefore material surrounding the crack tip is under elastic deformation. Hence, a crack with a depth of 10mm and 15mm would be stable and would not yield cleavage break.

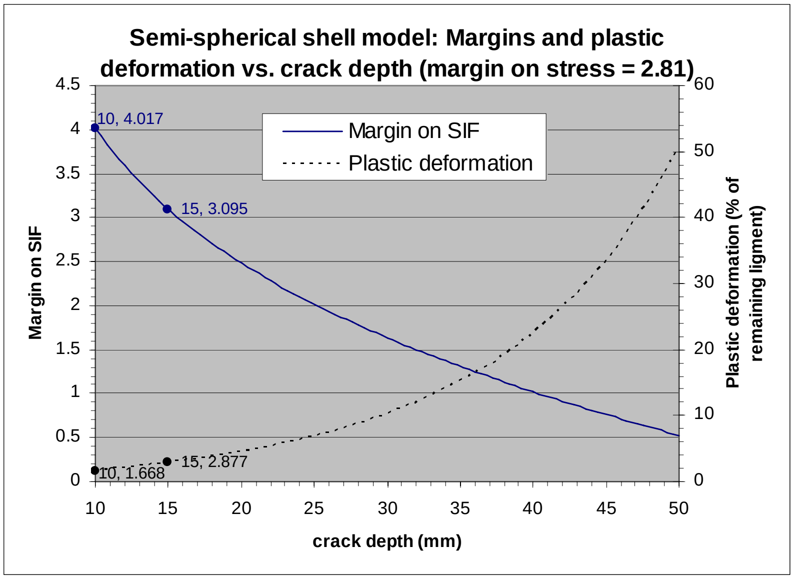

Figure 8 Analysis results according to semi-spherical shell model

6. OPEX

Operational experience (OPEX) has shown that vessel attachment weld indications are related to manufacturing of welds, the initiation sites are localized, and the depth is shallow in nature. Crack indications of such characteristics normally have no structural integrity significance.

7. Recommendations

Disposition of the two crack indications are recommended as follows. Firstly, a volumetric measurement of crack size, depth in particular, should be performed if no repair activities are planned. The measured crack sizes should be shallow and smaller than the calculated critical crack size. If repair by grinding is to be scheduled, crack depth should be estimated by recording how much material is to be removed. The estimated crack depth should be shallow and smaller than the calculated critical crack size. In both cases, continued service is recommended provided that acceptance requirements (ASME code Section XI subarticles IWB-3132.1, IWA-1400, IWA-2220 and IWA-6230) are satisfied.

8. Conclusions

Two calculation models addressed in this paper, the beam-bending model and the semi-spherical shell model, were used to establish the maximum allowable depth of cracks in the SG upper lateral support lug attachment welds. Based on the results of the analysis, cracks with a depth up to 15mm have both margin on stress intensity factor and margin on stress greater than one, hence considered to be stable and would not yield cleavage break. Grinding removal of cracks smaller than 15mm are allowed and return-to-service after crack removal is recommended.

The two crack indications were removed by grinding, and the actual crack depths were measured to be less than 1 mm. Since the crack indications are much lower than the calculated critical crack depth, it can be concluded that cracks are shallow, have no significant impact on the integrity of the attachment welds, and meets the crack size criterion for continued service. Follow-up inspections on the attachment welds in ensuing outages were performed and no further crack indications were discovered. This exercise of dispositioning crack indications demonstrates that the cracks at attachment welds of SG support lugs are structurally insignificant; the cause of such cracking is believed to be due to manufacturing of welding; the occurrence of such cracking is not related to operations and is isolated; grinding removal of such shallow cracks is proved to be effective and no reoccurrence of such cracks is reported.

9. Acknowledgement

Ontario Power Generation (OPG) is acknowledged to allow the publication of this paper. The assistance from Mr. Erik Cartar and Dr. Mike Stojakovic of OPG is also acknowledged.

10. References

[1] American Society of Mechanical Engineers, "ASME Boiler & Pressure Vessel Code – Section XI", 2000 edition with 2002 addenda, Three Park Avenue, New York, NY 10016-5990, 2002

[2] Paras, D. B., "Darlington design manual – main system", Ontario Power Generation document NK38-DM-36100 R002, August 27, 2004, pages 16-17

[3] U.S. Nuclear Regulatory Commission, "Pipe fracture encyclopedia –volume 3 pipe fracture test data", U.S. Nuclear Regulatory Commission, Washington D.C. 20555, 1997

[4] Tada, H., Paris P. C. and Irwin G. R., "The stress analysis of cracks handbook" 3rd edition, ASME Press, Three Park Avenue, New York, NY 10016, 2000 (pages 52 and 55)

[5] Timoshenko, S. P. and Woinowsky-Krieger, S., "Theory of plates and shells" 2nd edition, McGraw-Hill Book International Editions, December 1969. (page 484)

[6] Roy, S. and Sedmihradsky, P., "Darlington NGD steam generator baseline document", Appendix A of "Darlington steam generator life cycle management plan", Ontario Power Generation document NK38-PLAN-33110-00001, R02.